THE JOURNAL OF PHYSICAL CHEMISTRY B

Article

Cite This: J. Phys. Chem. B 2019, 123, 4108−4117

pubs.acs.org/JPCB

Exploring the Importance of Surface Diffusion in Stability of Vapor-Deposited Organic Glasses

Published as part of The Journal of Physical Chemistry virtual special issue "Young Scientists".

Subarna Samanta, Georgia Huang, Gui Gao, Yue Zhang, Aixi Zhang, Sarah Wolf, Connor N. Woods, Yi Jin, Patrick J. Walsh, and Zahra Fakhraai*

Department of Chemistry, University of Pennsylvania, Philadelphia, Pennsylvania 19104-6323, United States

Supporting Information

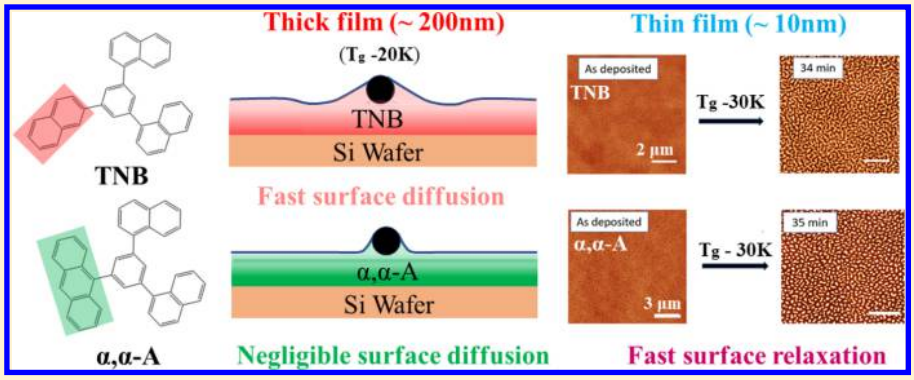

ABSTRACT: Stable glasses are formed during physical vapor deposition (PVD), through the surface-mediated equilibration process. Understanding surface relaxation dynamics is important in understanding the details of this process. Direct measurements of the surface relaxation times in molecular glass systems are challenging. As such, surface diffusion measurements have been used in the past as a proxy for the surface relaxation process. In this study, we show that the absence of enhanced surface diffusion is not a reliable predictor of reduced ability to produce stable glasses. To demonstrate, we have prepared stable glasses (SGs) from two structurally similar organic molecules, 1,3-bis(1-naphthyl)-5-(2-naphthyl)benzene (TNB) and 9-(3,5-di(naphthalen-1-yl)phenyl)anthracene (α,α-A), with similar density increase and improved kinetic stability as compared to their liquid-quenched (LQ) counterparts. The surface diffusion values of these glasses were measured both in the LQ and SG states below their glass transition temperatures (T_gs) using gold nanorod probes. While TNB shows enhanced surface diffusion in both SG and LQ states, no significant surface T_g diffusion is observed on the surface of α,α-A within our experimental time scales. However, isothermal dewetting experiments on ultrathin films of both molecules below T_g indicate the existence of enhanced dynamics in ultrathin films for both molecules, indirectly showing the existence of an enhanced mobile surface layer. Both films produce stable glasses, which is another indication for the existence of the mobile surface layer. Our results suggest that lateral surface diffusion may not be a good proxy for enhanced surface relaxation dynamics required to produce stable glasses, and thus, other types of measurements to directly probe the surface relaxation times may be necessary.

INTRODUCTION

Enhanced surface mobility[1−5] can affect the properties of glassy materials at nanoscale compared to their bulk counterparts.[6−10] This can significantly impact their end-uses which include coatings, drug delivery, nanoimprinting lithography,[11] membranes[12] and organic electronics applications.[13−17] In thin polymeric and organic glass materials, this liquid-like surface layer has been shown to alter material properties, such as the glass transition temperature (T_g),[18−22] aging rate,[23−27] and mechanical properties.[28−32]

In molecular glassformers, surface mobility has been primarily estimated through measurements of surface diffusion, particularly at temperatures below T_g.[33−36] It has been shown that the enhanced surface diffusion can impact the crystal growth process,[37−39] increasing the crystal growth rate even below T_g[40] and rendering the development of amorphous pharmaceutical drugs difficult. Furthermore, enhanced surface diffusion, and more generally the enhanced surface mobility, has been linked to the ability to form stable glasses (SG) through physical vapor deposition (PVD).[41−45]

Vapor-deposited stable glasses, first discovered by Ediger and co-workers,[46] have properties that are analogous to those of liquid-quenched (LQ) glasses that have been aged for thousands or millions of years.[47,48] They show better thermal

Received: January 31, 2019
Revised: April 17, 2019
Published: April 18, 2019

DOI: 10.1021/acs.jpcb.9b01012
J. Phys. Chem. B 2019, 123, 4108−4117

stability,[46,48] increased density,[49] higher modulus,[50,51] and improved kinetic[52,53] and photostability,[54,55] as well as other superior material properties.[56,57] These glasses are produced by exploiting the enhanced mobility of the surface molecules. When vapor depositing a material at a slow rate, on a temperature-controlled substrate kept below T_g, surface-mediated equilibration (SME) allows the incoming molecules to find more stable states before being buried into a quenched out-of-equilibrium state. Since SME is a kinetic process, many SG properties, such as density and thermal/kinetic stability, can be tuned based on the deposition rate and the deposition temperature.[57−63] Similarly, there is strong evidence that the structure of the liquid at the free surface may help template the glass structure, resulting in anisotropic and optically birefringent states.[63−67]

While stable glasses have potential applications in various fields, the details of the SME process and the exact formation mechanism of SGs are not fully understood. It is commonly understood that the enhanced diffusion of molecules at the surface layer allows the molecules to more rapidly sample configurations at the free surface and find states with lower fictive temperatures (T_f) in the potential energy landscape.[43,68] In molecules that can form hydrogen bonds, it has been demonstrated that the increasing hydrogen bond strength can result in slower surface diffusion, reducing the ability to form SGs.[69−74] However, this correlation is not perfect, and it has been noted in a recent study by Chen et al.[73] that other factors such as the size of the molecules, the mobility gradient within the film, and the extent of the intermolecular interaction are also important besides the surface diffusion coefficient. Consistent with this picture, recent computer simulations mimicking the experimental vapor deposition procedure have observed both enhanced diffusion of particles on the surface[45,75] and increased stability.[43,64,68] These simulations also demonstrate significant rearrangements below the immediate free surface.[45]

In a recent study, we used Tobacco Mosaic virus[35] to directly probe the diffusion at the surface of stable glasses formed of *N*,*N*′-bis(3-methylphenyl)-*N*,*N*′-diphenylbenzidine (TPD) molecule and demonstrated that the layer at the free surface may have dynamics that are decoupled from the bulk of the glass[19] and thus will likely not contribute to the formation of stable states.[76] As such, surface diffusion is at best a proxy for the enhanced dynamics of layers underneath the free surface layer. Using coarse-grained simulations,[45] we have also recently demonstrated that significant rearrangement can occur in layers below the immediate free surface, even for molecules that do not show significantly enhanced surface diffusion.

In this study, we provide an experimental example of a molecular glass system (*α*,*α*-A), where lateral surface diffusion is not observed, but the molecule can still form SGs relatively similar to SGs formed by a similar molecule TNB. Furthermore, we demonstrate that, in the ultrathin film (∼10 nm) state, both TNB and *α*,*α*-A show enhanced dewetting rates below T_g, a strong indication of the existence of a mobile surface layer with enhanced dynamics. The results show that while lateral surface diffusion can be a good proxy for the enhanced surface mobility, its absence does not necessarily mean that the surface dynamics are not enhanced. Our study suggests that direct probes of the surface relaxation dynamics need to be developed to investigate the relationship between the surface mobility and stable glass formation. Ultrathin film dewetting may provide another convenient proxy if feasible. We will explore this latter option in detail in our future studies.

EXPERIMENTAL DETAILS

The synthesis and bulk characterization of both 1,3-bis(1-naphthyl)-5-(2-naphthyl)benzene (TNB) and 9-(3,5-di(naphthalen-1-yl)phenyl)anthracene (*α*,*α*-A) molecules have been described in our previous publication.[77] The glass transition temperatures, T_g, of these molecules were measured by differential scanning calorimetry (DSC Q2000, TA Instruments) using hermetically sealed aluminum pans at a cooling at a rate of 10 K/min (Figure S7 of the online supporting info (Supporting Information)). The T_g values measured by DSC are $T_{g(\mathrm{TNB})} = 343 \pm 1$ K and $T_{g(\alpha,\alpha-\mathrm{A})} = 363 \pm 1$ K. Films of both molecules were prepared as amorphous thin films (∼200 nm thick) on Si substrate with a native oxide layer, in a custom-built ultrahigh vacuum chamber (base pressure $\sim 3 \times 10^{-7}$ Torr), using a typical deposition rate of 0.2 nm/s at 298 K. Deposition rates were monitored using a quartz crystal microbalance (Inficon Instruments). For ultrathin films of these molecules (∼10−12 nm), a slower deposition rate of 0.02−0.04 nm/s was used instead. More details of the chamber setup and the deposition process can be found in the Supporting Information (Figure S2).

The thickness of these films were measured using a variable-angle spectroscopic ellipsometer (SE, J. A. Woolam, M-2000 V) at 70° incident angle. A three-layer model which consists of a silicon layer, a native silicon oxide layer (1 nm in thickness) and a uniaxial anisotropic Cauchy model was used to fit the measured spectroscopic angles $\psi(\lambda)$ and $\Delta(\lambda)$ in the wavelength region of 500−1600 nm (Supporting Information, Figure S3). The thickness of the as-deposited films was monitored by SE during heating, isothermal transformation to supercooled liquid (SCL), and cooling back to LQ glass; at a cooling and heating rate of 10 K/min. A Linkam temperature-control stage (THMS600 V) was used to monitor and control the temperature. The isothermal transformation temperature of T_g + 25 K was used (more details are given in the Supporting Information and Figure S4).

Surface diffusion measurements were performed using long-aspect ratio gold nanorods (length/diameter = AR = ∼8) with a typical diameter of 22 ± 1 nm (Figure S8). These gold nanorods were coated with a cationic surfactant, hexadecyltrimethylammonium bromide (CTAB). The gold nanorod (AuNR) solution (Nanopartz Inc.) was spun-cast onto the surface of thick (∼200 nm) *α*,*α*-A and TNB films to achieve a dilute and uniform distribution of AuNRs. After spin coating, the film surface was further treated with Milli-Q water, which helps remove the excess CTAB from the film surface. The advantage of using AuNRs instead of previously used Tobacco Mosaic virus (TMV)[19,35,76] is thermal stability at higher temperatures and a reduced number of residual contaminants on the surface.

Isothermal annealing at $T < T_g$ was performed with a custom thermoelectric heating-stage and a thermistor (Oven industries TS91−10K) calibrated with three melting point standards (purchased from Sigma-Aldrich) ranging from 320 to 353 K (details in the Supporting Information). To track the evolution of the surface response to the nanorod perturbation, tapping mode atomic force microscopy (AFM) imaging (Noncontact AFM tips from Budget Sensors, Tap-300G, resonance frequency 300 kHz, tip radius of curvature <10 nm, force constant 40 N/m, Agilent 5420 AFM) was performed at

DOI: 10.1021/acs.jpcb.9b01012
J. Phys. Chem. B 2019, 123, 4108−4117

various isothermal annealing temperatures ranging from 303 to 358 K.

RESULTS

Formation of Stable Glasses by TNB and α,α-A. Figure 1 shows how the thicknesses of TNB and α,α-A vapor-deposited glass films change during temperature cycling. The as-deposited films were heated from 298 K to T_g + 25 K at a rate of 10 K/min. After the transformation into the supercooled liquid (SCL) state is complete, samples were cooled back to 298 at 10 K/min and the T_g was measured. The measured T_g values using ellipsometry are $T_{g(TNB)}$ = 342 ± 1 K and $T_{g(\alpha,\alpha-A)}$ = 363 ± 1 K, respectively. These values are adapted as T_g for the rest of the manuscript. The differences in the densities of the SG and LQ states were measured at 298 K to be $\Delta\rho_{(TNB)}$ = 1.41 ± 0.05% and $\Delta\rho_{(\alpha,\alpha-A)}$ = 1.36 ± 0.03%, respectively (Figure 1), which is consistent with our previously published results[56,61,63] (direct comparisons shown in Figure S6 of the Supporting Information). The fictive temperatures of each of these systems were also obtained from the data shown in Figure 1 by extrapolating the supercooled liquid line to the stable glass line. The values of the fictive temperatures were measured to be $T_{f(TNB)}$ = 309 ± 1 K and $T_{f(\alpha,\alpha-A)}$ = 329 ± 1 K, respectively, corresponding to an estimated age of ∼140 years for TNB and ∼68 years for α,α-A respectively, based on our previously reported values of fragility for these two systems along with Arrhenius extrapolation.[61] These results indicate that both TNB and α,α-A form reasonably similar stable glasses under these deposition conditions.

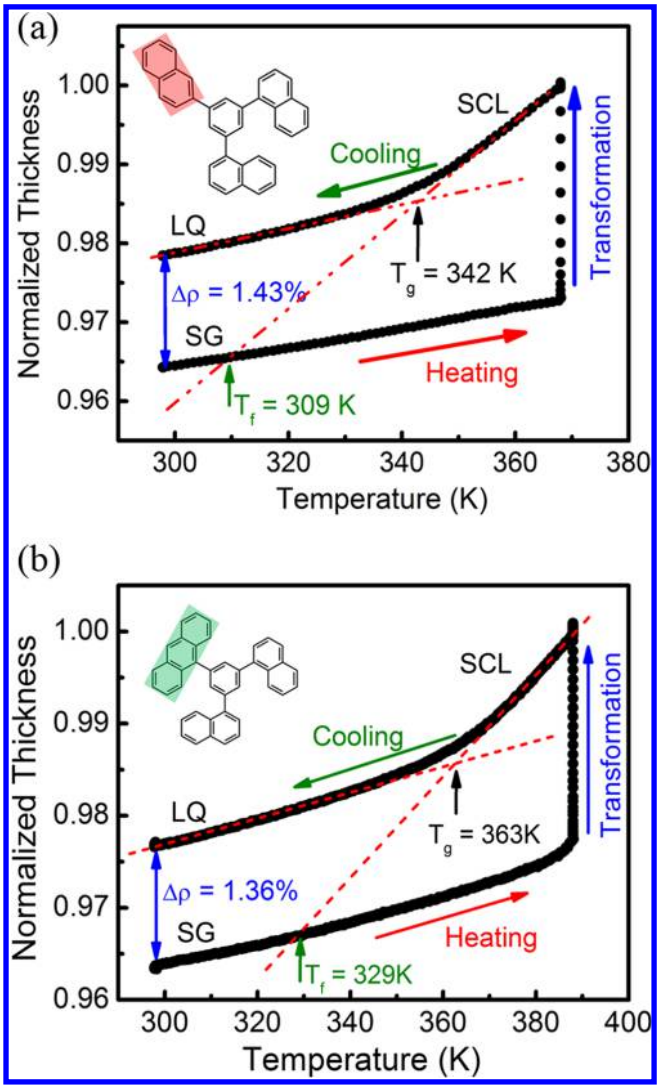

Figure 1. (a) Normalized film thickness vs temperature for a 191 nm thick film of stable glass TNB being transformed into LQ glass. (b) Normalized film thickness vs temperature for a 170 nm thick film of stable glass α,α-A being transformed into LQ glass. Both films were deposited at 298 K and at a rate of 0.2 nm/s. Heating and cooling rates were 10 K/min, and SGs were transformed isothermally at 25 K above their respective T_gs.

Surface Diffusion Measurement of TNB and α,α-A. For measurements of the surface diffusion, long-aspect-ratio AuNRs (AR ∼ 8) were placed on the surface. The mobile molecules on the surface respond to this perturbation by forming a meniscus around the AuNRs. At temperatures above T_g, this will result in the embedding of the AuNR. However, well below T_g, the motion of the molecules are diffusive on the free surface and the rest of the system is in a rigid glassy state. Thus, the rods stay on the surface (constant height) while the meniscus is being formed. As demonstrated in our earlier publications,[19,35,76] if the aspect ratio of the rod is long enough (semi-two-dimensional flow), for a purely surface diffusive process, the meniscus evolution follows a self-similar shape with space and time ($x/t^{1/4}$) that can be described by the Mullins model[78] as

$$\frac{\partial h(x,t)}{\partial t} = -\frac{D_s \gamma \Omega^2 \nu}{kT}\frac{\partial^4 h(x,t)}{\partial x^4} \quad (1)$$

where x is the distance from the center of the rod along the direction normal to it is axis (as shown in line profiles of Figure 2), D_s is the surface diffusion coefficient, γ is the surface tension, Ω represents the molecular volume, and ν is related to the thickness of the surface layer, which was assumed to be one-molecule thick. In the self-similar regime, the prefactor in this equation can be used to estimate the value of the surface diffusion D_s.

The evolution of the meniscus around the AuNRs at various temperatures and various annealing times below the respective T_g of each molecule was studied using tapping mode AFM. Figure 2 shows time-lapsed AFM images of the surface of the two molecules, after the placement of AuNRs on the surface, and their corresponding graphs of profiles of the menisci formed at each time point. Parts a and b of Figure 2 show that for TNB, when the film is held below T_g (T_g − 19 K), the meniscus grows rapidly with annealing time, such that within ∼30 min the width of the meniscus grows to about 350 nm, for the 22 nm AuNRs. In contrast, for α,α-A during isothermal annealing at a similar relative temperature of T_g − 20 K there is no apparent meniscus growth even after 34 h of annealing. Similar measurements were carried out in the temperature range of T_g − 14 K to T_g − 39 K for TNB and T_g − 5 K to T_g − 30 K for α,α-A in both LQ and SG states. For all temperatures, rapid meniscus growth was observed on the TNB surface, while little to no growth was observed on the α,α-A surface.

To explore whether the menisci formed around TNB are self-similar, indicating a surface diffusion process, the profiles around the AuNRs at different annealing times were plotted as a function of reduced distance, $x/t^{1/4}$, where x is the distance from the AuNR's center in the direction normal to the axis of

DOI: 10.1021/acs.jpcb.9b01012
J. Phys. Chem. B 2019, 123, 4108−4117

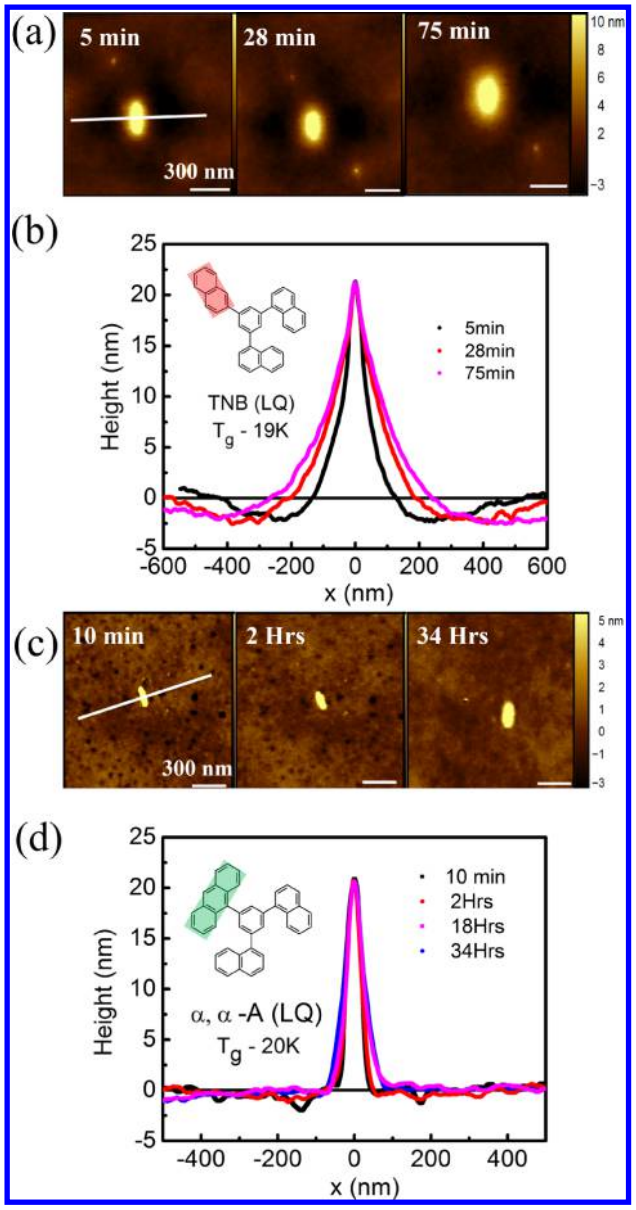

Figure 2. (a) AFM topography images of the evolution of the meniscus around gold nanorods with time during isothermal annealing of a 144 nm thick LQ film of TNB at T_g−19 K (323 K). (b) Height profiles extracted from the AFM images in part a showing the growing width of the meniscus. (c) AFM topography images of the evolution of the meniscus around AuNRs with time during isothermal annealing of a 170 nm thick LQ film of α,α-A at T_g − 20 K (343 K). (d) Height profiles extracted from the AFM images in part c showing the relatively constant width of the meniscus with time. The scale bar in all AFM images is 300 nm.

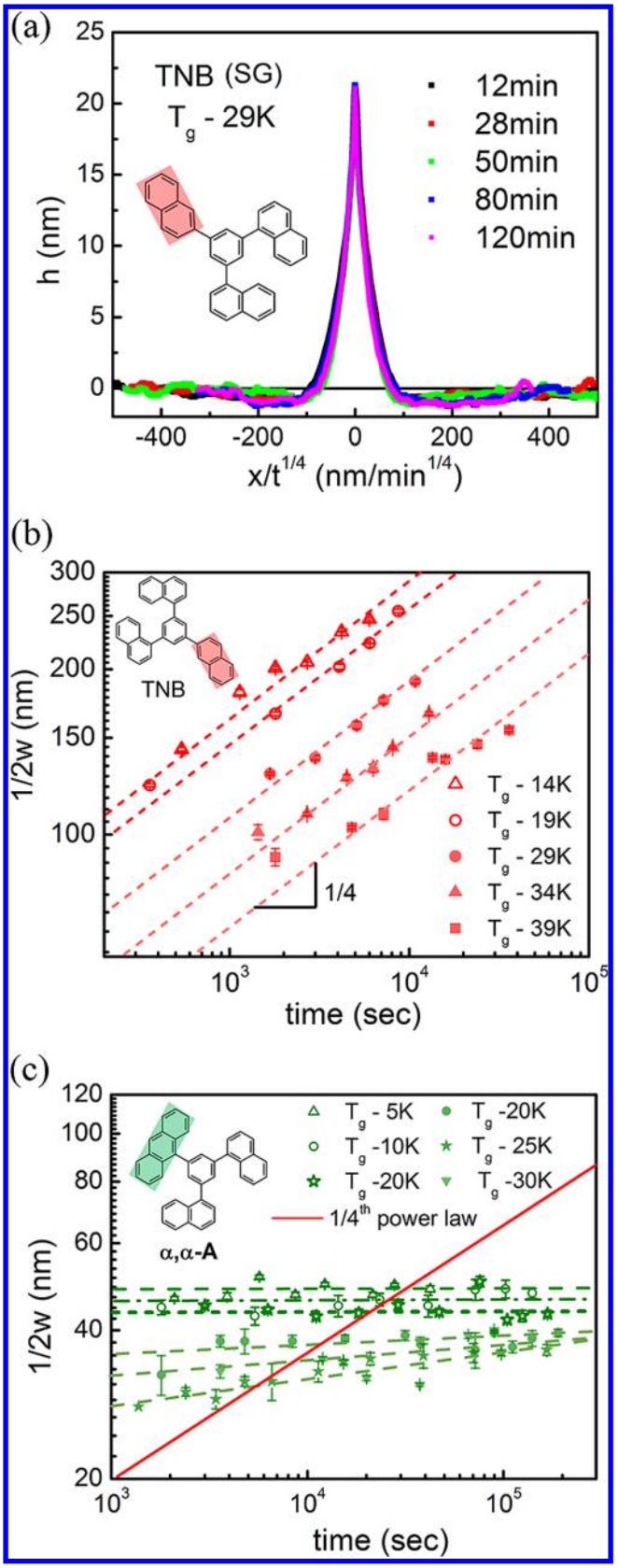

Figure 3. (a) Meniscus profiles across AuNRs on the surface of a 178 nm SG film of TNB held at a temperature of T_g − 29 K (313 K) as a function of scaled distance from the meniscus center $x/t^{1/4}$. The excellent overlap of the menisci indicates self-similarity of the profile. (b) Half profile width (w) as measured at a height of h = 2 nm from the film surface, vs time at various annealing temperatures. Open

the rod. As shown in Figure 3a for a stable glass film of TNB held at T_g − 29 K, all profiles collapse to a single master curve reasonably well within the experimental noise (actual profiles shown in Figure S9 of the Supporting Information). These results indicate that, within the error of these experiments, the $^1/4$ power-law is held for these profiles and the evolution of the meniscus is governed by the surface diffusion, as shown in eq 1. This self-similar behavior has been observed previously in experiments with another small molecule, TPD.[35,76]

Temperature Dependence of the Surface Diffusion Process. Following the procedure detailed in our previous

DOI: 10.1021/acs.jpcb.9b01012
J. Phys. Chem. B 2019, 123, 4108−4117

Figure 3. continued

symbols show meniscus growth on the LQ glass surface, while solid symbols show measurements on the SG glass surface. The dashed lines are fits to the data with a constant slope of $^1/_4$. (c) Half profile width (w) as measured at a height of h = 2 nm from the film surface, vs time at various annealing temperatures for α,α-A. Open symbols show the meniscus growth on the LQ glass surface, while solid symbols show measurements on the SG glass surface. The red solid line shows a line with a slope of $^1/_4$.

publications[35,76] the profile widths were measured at various annealing times for TNB at temperatures ranging from T_g − 14 K to T_g − 39 K as shown in Figure 3b. The fit lines indicate the one-fourth power law, and it is evident that for TNB, even at T_g − 39 K, fast surface diffusion can be observed. These observations are consistent with the previously reported grating decay measurements.[33,37] Figure 3c depicts the same data for α,α-A at a few measured temperatures below T_g. It can be seen from Figure 3c that there is almost no change in the profile width as a function of time. For comparison, the line that corresponds to the one-fourth power law is also shown, indicating that the surface mobility is at best subdiffusive if not absent.

DISCUSSIONS

Surface Diffusion of Liquid-Quenched TNB. As described in our earlier publications,[35,76] the data shown in Figure 3b can be used to estimate the value of the surface diffusion (D_s) on the TNB surface at various temperatures. To do so, we note that the intercept values extracted at various annealing temperatures from Figure 3b are proportional to D_s through the prefactor shown in eq 1. Using our previous modeling[35] and values of the parameters reported in ref 37 (also listed in the Supporting Information), surface diffusion at each temperature can be calculated. These values are shown in Figure 4 along with the results of the surface diffusion coefficient of TNB obtained previously using surface grating decay measurements.[37]

Focusing on D_s values measured on the liquid quenched (LQ) glass surface, Figure 4 shows that the values measured using AuNRs probe agree well with the data obtained by the grating decay method developed by Yu's group.[37] Due to the relatively small lateral size of the AuNRs compared to the gratings, our measurements can be readily extended to lower temperatures. Our experiments show that down to T_g − 39 K, D_s remains Arrhenius with an activation energy of 115 ± 7 kJ/mol, which is similar to the reported value in ref 37. This is a much lower activation barrier than the bulk activation energy, which is measured to be around 360 kJ/mol at T_g based on the data in ref 37. This means that as the temperature is decreased the difference between the values of D_s and D_v grows, consistent with previous measurements on various molecules.[33,35,37] While at T_g the D_s is only ∼7 decades faster than D_v, at the lowest measured temperature, T_g − 39 K (303 K), the difference can be 12−20 orders of magnitude depending on the method of extrapolation (more details in the Supporting Information, Table S1).

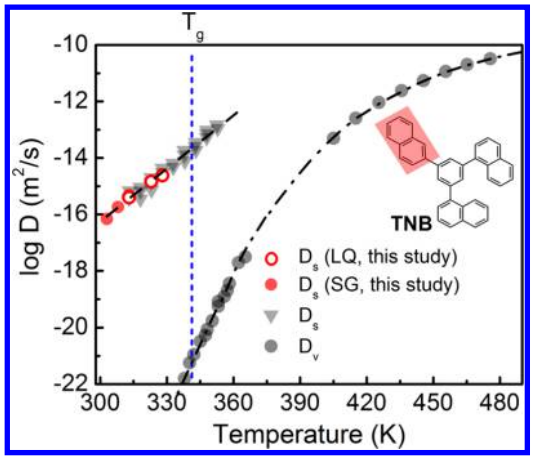

Figure 4. Surface (D_s) and bulk (D_v) diffusion coefficients of TNB. The open red symbols represent data obtained from LQ glass surfaces and the solid red points are measured on SGs. Data points in gray are D_s (triangles) and D_v (circles) values obtained from ref 37.

We also note that while an earlier report by Daley et al. using gold nanospheres[36] showed enhanced D_s for TNB, their values are inconsistent with either grating decay measurements[37] or the results of this study. For nanospheres, there are two curvatures around a nanosphere, one positive and one negative, that go to zero or infinity, respectively, at the center of the sphere, resulting in a singularity. Due to this singularity, the authors only reported estimated values of the surface diffusion.[36] The small curvatures around the nanospheres can also potentially affect the resolution of the AFM imaging, which becomes harder to detect at lower temperatures where the meniscus is small, likely resulting in temperature-dependent errors in evaluation of the temperatures. In contrast, for the one-dimensional problem of rods, there is only one curvature, resulting in self-similar profiles that greatly improve the confidence of the profile shapes.[35] Furthermore, the $^1/_4$ power law can be directly verified using time-dependent profiles, such as the data shown in Figure 3b, reducing the effect of noise in the data presented in this manuscript.

Surface Diffusion of Stable Glass TNB, and Its Decoupling from Bulk Dynamics. The nanorod probe is uniquely capable of directly measuring D_s on the surface of stable glass films.[76] As shown in Figure 4, D_s values measured on the SG surface are the same, within the experimental error, as the D_s values measured on the LQ glass surface. At T_g − 29 K, where overlapping experiments were performed, the raw data shown in Figure 3 and in the Supporting Information (Figure S10) are also identical within our experimental error. Due to the significant "aging" of the SG film, the extrapolated D_v for the SG glass with a fictive temperature of T_g − 33 K, as is the case here, is roughly 13 orders of magnitude slower than even those on the LQ glass surface.[79,80] However, the surface diffusion values are apparently unaffected by this large change in the effective bulk diffusion coefficient (and thus relaxation time). This is a strong evidence that the lateral diffusion at the immediate free surface, D_s, is decoupled from the bulk dynamics.

This observation is consistent with previous experiments that observed that the surface diffusion remains invariant while bulk dynamics are varied by orders of magnitude, either through preparation of SGs with varying fictive temperatures,[76] physical aging,[76,81] or preparation of ultrathin films with enhanced dynamics.[19]

While these measurements have only been performed on a handful of molecules and systems, they indicate that when enhanced surface diffusion is present, D_s and D_v may decouple. One explanation for this observation is the presence of a large

DOI: 10.1021/acs.jpcb.9b01012
J. Phys. Chem. B 2019, 123, 4108−4117

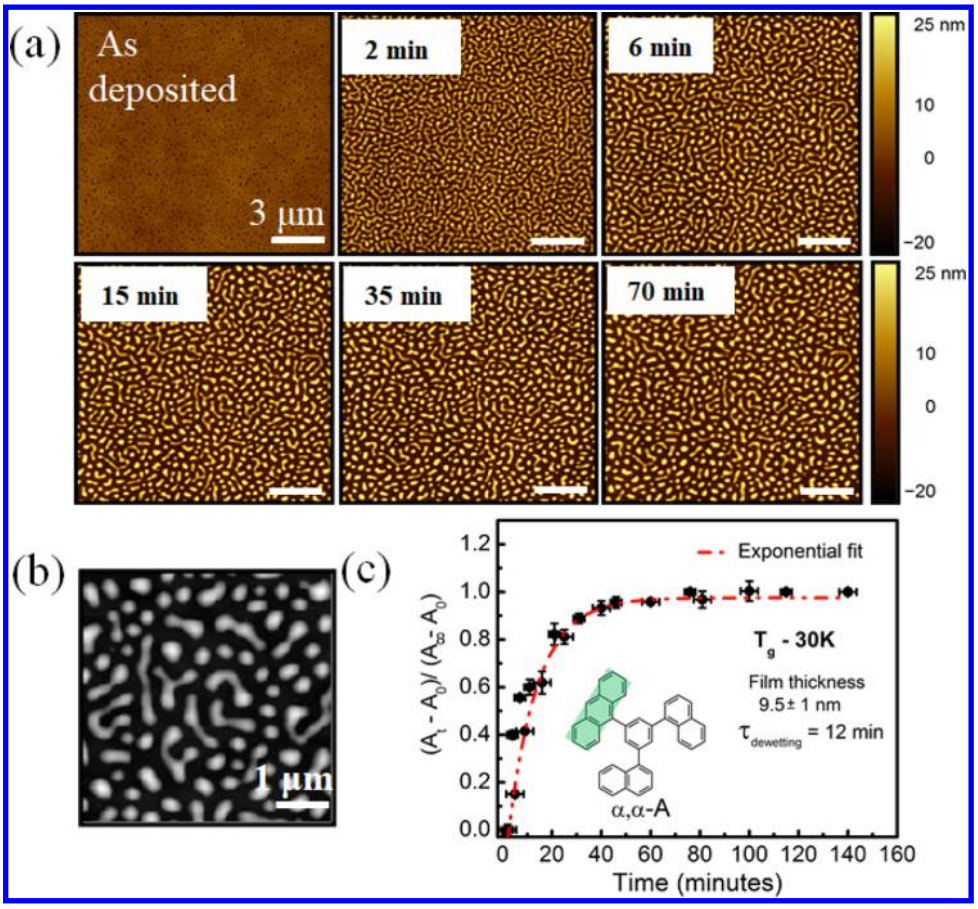

Figure 5. (a) Evolution of the morphology of a 10 ± 1 nm thick α,α-A film during isothermal dewetting at T_g − 30 K (333 K). The scale bar is 3 μm. All films were deposited at 297 K with a deposition rate of 0.02 nm/s. (b) A height threshold is set using ImageJ software to calculate the dewetted area (black). (c) Dewetted area as a function of time obtained from the AFM images in part a after setting an appropriate height threshold.

dynamical difference between D_s and D_v, which can be 6−7 decades at T_g, increasing as the temperature is lowered further below T_g. This large dynamical range can result in decoupling between the dynamics at the free surface and the bulk of the film. If true, one can then ask whether lowering this dynamical range can allow a system to stay coupled, such that decreasing the bulk fictive temperature would result in decreasing the surface diffusion. The only current example of such a system, where direct measurements are available, is in ultrathin TPD films where the bulk dynamics themselves are enhanced.[19] The results of this study showed a dynamical decoupling despite decreasing dynamical differences. In contrast, indirect crystal growth measurements on a pharmaceutical drug molecule, celecoxib, has shown that the crystal growth rates are different for SG and an LQ glass states.[82] Surface diffusion studies on this material would be an interesting test for the generality of this explanation. Another approach would be to extend the studies in this report to a range of molecules with varying molecular weights where the D_s for the liquid quenched glass has been previously measured and has been shown to become closer to D_v as the molecular weight is increased.[34] This will be the focus of our future studies.

Absence of Surface Diffusion in α,α-A. As mentioned above, the molecular weight (M_w) of the molecule can affect the surface diffusion coefficient for small molecules and even for low molecular weight polymers.[34] Since α,α-A has a higher molecular weight (M_w = 506.6 g/mol) compared to TNB (M_w = 456.6 g/mol), α,α-A is expected to have a slightly lower surface diffusion coefficient (Figure S11 of the Supporting Information). On the basis of the temperature dependence of D_s for TNB, we estimate the surface diffusion of TNB at T_g to be $D_{s(\mathrm{TNB})} \sim 2.5 \times 10^{-14}$ m^2/s. On the basis of the M_w dependence of D_s reported in ref 34 (Figure S11 of Supporting Information), the surface diffusion of α,α-A at T_g is estimated to be $D_{s(\alpha,\alpha\mathrm{A})} \sim 1.5 \times 10^{-14}$ m^2/s. However, clearly the surface diffusion of α,α-A is much slower than the estimated value, as we do not observe any significant meniscus formation around the AuNRs as shown in Figures 2 and 3. As we were not able to observe significant surface diffusion, we can only estimate an upper bound value for the surface diffusion coefficient of α,α-A at T_g, which is approximately $D_{s-(\alpha,\alpha-\mathrm{A})}(UB) = 10^{-18}$−$10^{-19}$ m^2/s, roughly 4−5 decades slower than the estimated value (details shown in Figure S11 of the Supporting Information).

The absence of the enhanced surface diffusion on α,α-A, for both LQ and SG glass states, is surprising. We hypothesize that this is due to pairing or aggregation of anthracenyl substituents on the free surface. We have previously shown that in both SG or LQ glasses, α,α-A molecules, as well as the anthracene substituents, are randomly oriented without any specific direction and without any significant coupling with their neighboring molecules.[63] However, at the free surface, it is possible for the anthracenyl groups to segregate to the free surface and orient normal to the surface. As such, it is more likely for these substituents to form pairs due to stronger π

DOI: 10.1021/acs.jpcb.9b01012
J. Phys. Chem. B 2019, 123, 4108−4117

interactions. Such aggregation on the free surface can result in the formation of larger clusters that can hinder the free surface diffusion.[45] As direct measurements of the orientation of these molecules at the surface are beyond our ability to resolve, future studies are required to evaluate this hypothesis.

Evidence of Enhanced Surface Dynamics in α,α-A. Given the absence of surface diffusion, it is surprising that α,α-A can still form stable glasses upon PVD, with stable glass states that are reasonably similar to that of TNB, as shown in Figure 1 and Figure S6. This is in contrast to previous studies of alcohols, where formation of hydrogen bonding at the free surface resulted in reduced ability to form stable glasses under similar conditions.[69,71,72] It was hypothesized that hydrogen bonding reduces surface diffusion/relaxation and thus the molecules are unable to find lower energy states to equilibrate. Measurements of surface diffusion are typically used as a proxy for enhanced surface relaxation dynamics, and thus are considered to be indicative of the ability to form stable glasses.[33,35,37] For molecules such as TNB and TPD, where enhanced surface diffusion is present, this may be correct to some extent. Whereas, the increased stability in α,α-A glasses as well as the presence of decoupling between D_s and D_v, as observed in both TPD and TNB, indicate that this proxy is an unreliable measure.

Another example of the decoupling between D_s and surface relaxation time, τ_s, can be found in polymeric systems with large molecular weights. In such systems, lateral surface diffusion is impossible due to chain entanglement at layers below the free surface. Nonetheless, significantly enhanced surface relaxation time (τ_s) is observed.[1,2,4,5] In polymeric systems, the enhanced surface mobility has been directly linked to the enhanced mobility in ultrathin films.[3,83−85] We have recently demonstrated that for molecular glass of TPD, a similar behavior can be observed, where enhanced surface mobility can result in lower T_g values as well as enhanced dewetting rates in films with thicknesses below 30 nm.[86] Since in small molecules the viscosity is directly proportional to the relaxation time (τ_α) of the system, the relaxation time of the thin film at the limit of zero thickness, obtained through viscosity (dewetting) measurements, is another good proxy for the surface relaxation time τ_s. Interestingly, the activation energy values obtained for τ_s for TPD in that study were lower than the measured activation energy values based on D_s and the two processes were shown to be decoupled from each other.[19]

To probe whether the thin film dynamics (as another proxy to surface relaxation times) are enhanced in TNB and α,α-A, we studied the dewetting kinetics in ultrathin films of these systems. Interestingly, the as-deposited films of both molecules showed evidence of dewetting on the silicon substrate, even during the deposition process at room temperature (297 K), indicating enhanced mobility in the thin film state, even though the thick films deposited at the same temperature can form stable glasses. Figure 5 shows the continued spinodal-like dewetting of a ∼10 nm film of α,α-A when held at T_g−30 K (333 K). Similar data for TNB is shown in the Supporting Information, Figure S12.

The dewetting pattern and time scales are similar to the values previously observed in TPD,[86] indicating similarly enhanced viscosity and thus τ_α values. While a full characterization of the dewetting kinetics and evaluation of the viscosity as a function of film thickness is beyond the scope of this study, the reasonably similar dewetting kinetics between TNB and α,α-A indicates that the two systems have similarly enhanced relaxation dynamics at their surface, that can propagate over a fairly long length scale of at least 10 nm. It is important to note that even at temperatures where the bulk forms a SG, thin films have enhanced mobility and can dewet, as is evident by dewetting during deposition. Thus, it is likely that, during the steady state deposition conditions, while the bulk of the glass is at a deeply quenched glassy state, the layers closer to the free surface (within ∼10 nm), can have different dynamics and possibly be faster than even the SCL glass. As such, the system is able to equilibrate, not just at the layer immediately at the free surface but well after it is buried under the flux of the incoming molecules.

The results of this study indicate that the immediate free surface dynamics as opposed to only the surface diffusion should be taken into account in predicting the stability of a PVD glass. However, it is also important to measure and understand the length scale over which the dynamics are modified and the extent of this modification. Both the degree of enhancement and the depth of enhanced dynamics are required to predict the ability of a molecule to form a stable glass. This is also consistent with recent coarse grained simulations that show rearrangement well below the free surface.[45] We are unaware of any experimental technique that can directly measure both of these quantities on the surface of SGs, but developing such techniques is an important future goal. In the absence of such techniques, dewetting experiments can potentially serve as a better proxy for enhanced surface dynamics than D_s measurements. For example, one can probe as whether enhanced dewetting rates can be observed in hydrogen-bonding systems or whether in those systems the strong network formation suppresses both D_s and τ_s, or possibly decreases the thickness of the mobile layer. Such future experiments can be important in verifying the utility of dewetting experiments for predicting the stable glass formation ability of a particular molecule.

CONCLUSION

In summary, we have investigated the stable glass formation of two structurally similar compounds, namely TNB and α,α-A, at room temperature. Stable glasses of these two compounds were found to be approximately 1.3−1.4% denser compared to their ordinary glass counterparts and similar in their fictive temperatures ($T_f = T_g - 33$ K). We studied the surface diffusion process of these two molecules in both liquid-quenched and stable glass forms. In accordance with previous reports, we found that on the liquid-quenched TNB glasses surface diffusion is faster than its bulk diffusion by orders of magnitude. The surface diffusion on the stable glass TNB surface was also measured and it was demonstrated to be the same as the LQ surface diffusion, indicating a decoupling of the bulk and surface diffusion processes. In contrast, we observed negligible surface diffusion for α,α-A within our experimental time scale, despite the fact that it is structurally similar to TNB. Both results indicate that D_s measurements are not an adequate proxy for surface relaxation measurements or predicting the ability of a molecule to form a stable glass.

To indirectly measure the enhanced surface relaxation dynamics in α,α-A, dewetting experiments were performed on ultrathin films of α,α-A well below bulk T_g. It was found that films as thick as ∼10 nm have significantly enhanced mobility compared to the bulk glass and that the TNB and α,α-A have reasonably similar dewetting kinetics at a similar

DOI: 10.1021/acs.jpcb.9b01012
J. Phys. Chem. B 2019, 123, 4108−4117

relative temperature compared to their bulk T_g. As such, compared to the D_s measurements, dewetting experiments provide a more accurate proxy for the enhanced surface mobility as well as the depth of the mobile surface layer that can both contribute to the process of stable glass formation. Direct probes of surface relaxation dynamics as opposed to D_s measurements should be developed in the future to better understand the process of stable glass formation.

■ ASSOCIATED CONTENT

Supporting Information

The Supporting Information is available free of charge on the ACS Publications website at DOI: 10.1021/acs.jpcb.9b01012.

Description of the ultrahigh vacuum chamber, ellipsometry, DSC measurement, data analysis, estimation of bulk diffusion coefficient of TNB, comparison of meniscus growth over time for LQ and SG TNB, and the dewetting kinetics of vapor-deposited TNB below T_g (PDF)

■ AUTHOR INFORMATION

Corresponding Author

*(Z.F.) E-mail: fakhraai@sas.upenn.edu.

ORCID

Yi Jin: 0000-0002-5633-8305

Patrick J. Walsh: 0000-0001-8392-4150

Zahra Fakhraai: 0000-0002-0597-9882

Notes

The authors declare no competing financial interest.

Biography

Zahra Fakhraai received her B.Sc. and M.Sc. degrees in physics from the Sharif University of Technology in Iran. She then joined Jamie Forrest's group at the University of Waterloo to study the dynamics of polymer thin films and surfaces (2003−2007), for which she received the American Physical Society's Padden award (2007). Zahra worked in Gilbert Walker's group at the University of Toronto (2008−2009) where she performed near-field infrared imaging of the structure and chemical composition of protein aggregates. She received an NSERC postdoctoral fellowship in 2009 and moved to Mark Ediger's lab at the University of Wisconsin—Madison to study properties of stable glasses (2009−2011). Zahra joined the Department of Chemistry at the University of Pennsylvania in 2011 where she is currently an Associate Professor and Graduate Chair with a secondary appointment at the Department of Chemical and Biomolecular Engineering. Her group at Penn combines experiments and modeling to explore the structure, dynamics, and optical properties of amorphous materials at nanometer length scale. A key aspect of these studies is to understand how surfaces and interfaces affect properties of amorphous materials and how these effects can be used to engineer novel packings of molecular glasses, polymers, composites, and biopolymers. Zahra is a member of the American Physical Society, the American Chemical Society, the Materials Research Society, and the American Association for the Advancement of Science. She is the recipient of the NSF Career Award (2014), a Sloan Fellowship in Chemistry (2015), the Journal of Physical Chemistry JPC-PHYS Lectureship Award (2017), and the APS Dillon Medal (2019).

■ ACKNOWLEDGMENTS

We gratefully acknowledge the funding for this work: NSF-DMREF-1628407 and the NSF Faculty Early Career Development (CAREER) Program award, Grant DMR-1350044.

■ REFERENCES

(1) Fakhraai, Z.; Forrest, J. Measuring the Surface Dynamics of Glassy Polymers. *Science* **2008**, *319*, 600−604.

(2) Paeng, K.; Swallen, S. F.; Ediger, M. Direct Measurement of Molecular Motion in Freestanding Polystyrene Thin Films. *J. Am. Chem. Soc.* **2011**, *133*, 8444−8447.

(3) Sharp, J.; Teichroeb, J.; Forrest, J. The Properties of Free Polymer Surfaces and Their Influence on The Glass Transition Temperature of Thin Polystyrene Films. *Eur. Phys. J. E: Soft Matter Biol. Phys.* **2004**, *15*, 473−487.

(4) Chai, Y.; Salez, T.; McGraw, J. D.; Benzaquen, M.; Dalnoki-Veress, K.; Raphaël, E.; Forrest, J. A. A Direct Quantitative Measure of Surface Mobility in a Glassy Polymer. *Science* **2014**, *343*, 994−999.

(5) Kim, H.; Cang, Y.; Kang, E.; Graczykowski, B.; Secchi, M.; Montagna, M.; Priestley, R. D.; Furst, E. M.; Fytas, G. Direct Observation of Polymer Surface Mobility via Nanoparticle Vibrations. *Nat. Commun.* **2018**, *9*, 2918.

(6) Baker, E. A.; Rittigstein, P.; Torkelson, J. M.; Roth, C. B. Streamlined Ellipsometry Procedure for Characterizing Physical Aging Rates of Thin Polymer Films. *J. Polym. Sci., Part B: Polym. Phys.* **2009**, *47*, 2509−2519.

(7) Sepúlveda, A.; Leon-Gutierrez, E.; Gonzalez-Silveira, M.; Rodríguez-Tinoco, C.; Clavaguera-Mora, M.; Rodríguez-Viejo, J. Accelerated Aging in Ultrathin Films of a Molecular Glass Former. *Phys. Rev. Lett.* **2011**, *107*, 025901.

(8) Yang, Z.; Lam, C.-H.; DiMasi, E.; Bouet, N.; Jordan-Sweet, J.; Tsui, O. K. Method to Measure the Viscosity of Nanometer Liquid Films From the Surface Fluctuations. *Appl. Phys. Lett.* **2009**, *94*, 251906.

(9) Zuo, B.; Tian, H.; Liang, Y.; Xu, H.; Zhang, W.; Zhang, L.; Wang, X. Probing the Rheological Properties of Supported Thin Polystyrene Films by Investigating the Growth Dynamics of Wetting Ridges. *Soft Matter* **2016**, *12*, 6120−6131.

(10) Bay, R. K.; Shimomura, S.; Liu, Y.; Ilton, M.; Crosby, A. J. Confinement Effect on Strain Localizations in Glassy Polymer Films. *Macromolecules* **2018**, *51*, 3647−3653.

(11) Ding, Y.; Ro, H. W.; Douglas, J. F.; Jones, R. L.; Hine, D. R.; Karim, A.; Soles, C. L. Polymer Viscoelasticity and Residual Stress Effects on Nanoimprint Lithography. *Adv. Mater.* **2007**, *19*, 1377−1382.

(12) Huang, Y.; Paul, D. Physical Aging of Thin Glassy Polymer Films Monitored by Gas Permeability. *Polymer* **2004**, *45*, 8377−8393.

(13) Ràfols-Ribé, J.; Will, P.-A.; Hänisch, C.; Gonzalez-Silveira, M.; Lenk, S.; Rodríguez-Viejo, J.; Reineke, S. High-Performance Organic Light-Emitting Diodes Comprising Ultrastable Glass Layers. *Sci. Adv.* **2018**, *4*, eaar8332.

(14) Yokoyama, D. Molecular Orientation in Small-Molecule Organic Light-Emitting Diodes. *J. Mater. Chem.* **2011**, *21*, 19187−19202.

(15) Osada, K.; Goushi, K.; Kaji, H.; Adachi, C.; Ishii, H.; Noguchi, Y. Observation of Spontaneous Orientation Polarization in Evapo-

rated Films of Organic Light-Emitting Diode Materials. *Org. Electron.* **2018**, *58*, 313−317.
(16) Wakamiya, A.; Nishimura, H.; Fukushima, T.; Suzuki, F.; Saeki, A.; Seki, S.; Osaka, I.; Sasamori, T.; Murata, M.; Murata, Y.; Kaji, H. On-Top π-Stacking of Quasiplanar Molecules in Hole-Transporting Materials: Inducing Anisotropic Carrier Mobility in Amorphous Films. *Angew. Chem., Int. Ed.* **2014**, *53*, 5800−5804.
(17) Ediger, M.; de Pablo, J.; Yu, L. Anisotropic Vapor-Deposited Glasses: Hybrid Organic Solids. *Acc. Chem. Res.* **2019**, *52*, 407−414.
(18) Keddie, J. L.; Jones, R. A.; Cory, R. A. Size-Dependent Depression of The Glass Transition Temperature in Polymer Films. *Eur. Phys. Lett.* **1994**, *27*, 59.
(19) Zhang, Y.; Fakhraai, Z. Decoupling of Surface Diffusion and Relaxation Dynamics of Molecular Glasses. *Proc. Natl. Acad. Sci. U. S. A.* **2017**, *114*, 4915−4919.
(20) Alcoutlabi, M.; McKenna, G. B. Effects of Confinement on Material Behaviour at the Nanometre Size Scale. *J. Phys.: Condens. Matter* **2005**, *17*, R461.
(21) Napolitano, S.; Glynos, E.; Tito, N. B. Glass Transition of Polymers in Bulk, Confined Geometries, and Near Interfaces. *Rep. Prog. Phys.* **2017**, *80*, 036602.
(22) Ediger, M.; Forrest, J. Dynamics Near Free Surfaces and The Glass Transition in Thin Polymer Films: a View to The Future. *Macromolecules* **2014**, *47*, 471−478.
(23) Huang, Y.; Paul, D. Physical Aging of Thin Glassy Polymer Films Monitored by Optical Properties. *Macromolecules* **2006**, *39*, 1554−1559.
(24) Pye, J. E.; Rohald, K. A.; Baker, E. A.; Roth, C. B. Physical Aging in Ultrathin Polystyrene Films: Evidence of a Gradient in Dynamics at The Free Surface and Its Connection to The Glass Transition Temperature Reductions. *Macromolecules* **2010**, *43*, 8296−8303.
(25) Shavit, A.; Riggleman, R. A. Physical Aging, The Local Dynamics of Glass-Forming Polymers Under Nanoscale Confinement. *J. Phys. Chem. B* **2014**, *118*, 9096−9103.
(26) Priestley, R. D.; Ellison, C. J.; Broadbelt, L. J.; Torkelson, J. M. Structural Relaxation of Polymer Glasses at Surfaces, Interfaces, and in Between. *Science* **2005**, *309*, 456−459.
(27) Priestley, R. D. Physical Aging of Confined Glasses. *Soft Matter* **2009**, *5*, 919−926.
(28) Stafford, C. M.; Harrison, C.; Beers, K. L.; Karim, A.; Amis, E. J.; VanLandingham, M. R.; Kim, H.-C.; Volksen, W.; Miller, R. D.; Simonyi, E. E. A Buckling-Based Metrology for Measuring the Elastic Moduli of Polymeric Thin Films. *Nat. Mater.* **2004**, *3*, 545.
(29) Liu, Y.; Chen, Y.-C.; Hutchens, S.; Lawrence, J.; Emrick, T.; Crosby, A. J. Directly Measuring the Complete Stress−Strain Response of Ultrathin Polymer Films. *Macromolecules* **2015**, *48*, 6534−6540.
(30) Torres, J. M.; Stafford, C. M.; Vogt, B. D. Elastic Modulus of Amorphous Polymer Thin Films: Relationship to The Glass Transition Temperature. *ACS Nano* **2009**, *3*, 2677−2685.
(31) Chung, P. C.; Glynos, E.; Sakellariou, G.; Green, P. F. Elastic Mechanical Response of Thin Supported Star-Shaped Polymer Films. *ACS Macro Lett.* **2016**, *5*, 439−443.
(32) Du, B.; Tsui, O. K.; Zhang, Q.; He, T. Study of Elastic Modulus and Yield Strength of Polymer Thin Films Using Atomic Force Microscopy. *Langmuir* **2001**, *17*, 3286−3291.
(33) Zhu, L.; Brian, C.; Swallen, S.; Straus, P.; Ediger, M.; Yu, L. Surface Self-diffusion of an Organic Glass. *Phys. Rev. Lett.* **2011**, *106*, 256103.
(34) Zhang, W.; Yu, L. Surface Diffusion of Polymer Glasses. *Macromolecules* **2016**, *49*, 731−735.
(35) Zhang, Y.; Potter, R.; Zhang, W.; Fakhraai, Z. Using Tobacco Mosaic Virus to Probe Enhanced Surface Diffusion of Molecular Glasses. *Soft Matter* **2016**, *12*, 9115−9120.
(36) Daley, C.; Fakhraai, Z.; Ediger, M.; Forrest, J. Comparing Surface and Bulk Flow of a Molecular Glass Former. *Soft Matter* **2012**, *8*, 2206−2212.
(37) Ruan, S.; Zhang, W.; Sun, Y.; Ediger, M.; Yu, L. Surface Diffusion and Surface Crystal Growth of Tris-naphthyl Benzene Glasses. *J. Chem. Phys.* **2016**, *145*, 064503.
(38) Powell, C. T.; Xi, H.; Sun, Y.; Gunn, E.; Chen, Y.; Ediger, M.; Yu, L. Fast Crystal Growth in O-terphenyl Glasses: a Possible Role for Fracture and Surface Mobility. *J. Phys. Chem. B* **2015**, *119*, 10124−10130.
(39) Sun, Y.; Zhu, L.; Wu, T.; Cai, T.; Gunn, E. M.; Yu, L. Stability of Amorphous Pharmaceutical Solids: Crystal Growth Mechanisms and Effect of Polymer Additives. *AAPS J.* **2012**, *14*, 380−388.
(40) Zhu, L.; Jona, J.; Nagapudi, K.; Wu, T. Fast Surface Crystallization of Amorphous Griseofulvin Below T_g. *Pharm. Res.* **2010**, *27*, 1558−1567.
(41) Ediger, M. D. Perspective: Highly Stable Vapor-Deposited Glasses. *J. Chem. Phys.* **2017**, *147*, 210901.
(42) Berthier, L.; Charbonneau, P.; Flenner, E.; Zamponi, F. Origin of Ultrastability in Vapor-Deposited Glasses. *Phys. Rev. Lett.* **2017**, *119*, 188002.
(43) Singh, S.; de Pablo, J. J. A Molecular View of Vapor Deposited Glasses. *J. Chem. Phys.* **2011**, *134*, 194903.
(44) Chua, Y.; Ahrenberg, M.; Tylinski, M.; Ediger, M.; Schick, C. How Much Time Is Needed to Form a Kinetically Stable Glass? AC Calorimetric Study of Vapor-Deposited Glasses of Ethylcyclohexane. *J. Chem. Phys.* **2015**, *142*, 054506.
(45) Moore, A. R.; Huang, G.; Wolf, S.; Walsh, P. J.; Fakhraai, Z.; Riggleman, R. A. Effects of microstructure formation on the stability of vapor-deposited glasses. *Proc. Natl. Acad. Sci. U. S. A.* **2019**, *116*, 5937−5942.
(46) Swallen, S. F.; Kearns, K. L.; Mapes, M. K.; Kim, Y. S.; McMahon, R. J.; Ediger, M. D.; Wu, T.; Yu, L.; Satija, S. Organic Glasses With Exceptional Thermodynamic and Kinetic Stability. *Science* **2007**, *315*, 353−356.
(47) Yu, H.; Tylinski, M.; Guiseppi-Elie, A.; Ediger, M.; Richert, R. Suppression of β Relaxation in Vapor-Deposited Ultrastable Glasses. *Phys. Rev. Lett.* **2015**, *115*, 185501.
(48) Kearns, K. L.; Swallen, S. F.; Ediger, M. D.; Wu, T.; Sun, Y.; Yu, L. Hiking Down The Energy Landscape: Progress Toward the Kauzmann Temperature Via Vapor Deposition. *J. Phys. Chem. B* **2008**, *112*, 4934−4942.
(49) Dalal, S. S.; Fakhraai, Z.; Ediger, M. D. High-Throughput Ellipsometric Characterization of Vapor-Deposited Indomethacin Glasses. *J. Phys. Chem. B* **2013**, *117*, 15415−15425.
(50) Kearns, K. L.; Still, T.; Fytas, G.; Ediger, M. High-Modulus Organic Glasses Prepared by Physical Vapor Deposition. *Adv. Mater.* **2010**, *22*, 39−42.
(51) Tangpatjaroen, C.; Bagchi, K.; Martínez, R. A.; Grierson, D.; Szlufarska, I. Mechanical Properties of Structure-Tunable, Vapor-Deposited TPD Glass. *J. Phys. Chem. C* **2018**, *122*, 27775−27781.
(52) Rodríguez-Tinoco, C.; Gonzalez-Silveira, M.; Ràfols-Ribé, J.; Lopeandía, A. F.; Rodríguez-Viejo, J. Transformation Kinetics of Vapor-Deposited Thin Film Organic Glasses: The Role of Stability and Molecular Packing Anisotropy. *Phys. Chem. Chem. Phys.* **2015**, *17*, 31195−31201.
(53) Whitaker, K. R.; Tylinski, M.; Ahrenberg, M.; Schick, C.; Ediger, M. Kinetic Stability and Heat Capacity of Vapor-Deposited Glasses of O-Terphenyl. *J. Chem. Phys.* **2015**, *143*, 084511.
(54) Qiu, Y.; Dalal, S. S.; Ediger, M. Vapor-Deposited Organic Glasses Exhibit Enhanced Stability Against Photodegradation. *Soft Matter* **2018**, *14*, 2827−2834.
(55) Qiu, Y.; Antony, L. W.; Torkelson, J. M.; de Pablo, J. J.; Ediger, M. Tenfold Increase in The Photostability of an Azobenzene Guest in Vapor-Deposited Glass Mixtures. *J. Chem. Phys.* **2018**, *149*, 204503.
(56) Dawson, K. J.; Kearns, K. L.; Ediger, M.; Sacchetti, M. J.; Zografi, G. D. Highly Stable Indomethacin Glasses Resist Uptake of Water Vapor. *J. Phys. Chem. B* **2009**, *113*, 2422−2427.
(57) Ràfols-Ribé, J.; Dettori, R.; Ferrando-Villalba, P.; Gonzalez-Silveira, M.; Abad, L.; Lopeandía, A. F.; Colombo, L.; Rodríguez-Viejo, J. Evidence of Thermal Transport Anisotropy in Stable Glasses

DOI: 10.1021/acs.jpcb.9b01012
J. Phys. Chem. B 2019, 123, 4108−4117

of Vapor Deposited Organic Molecules. *Phys. Rev. Mater.* **2018**, *2*, 035603.
(58) Kearns, K. L.; Swallen, S. F.; Ediger, M.; Wu, T.; Yu, L. Influence of Substrate Temperature on The Stability of Glasses Prepared by Vapor Deposition. *J. Chem. Phys.* **2007**, *127*, 154702.
(59) Kearns, K. L.; Krzyskowski, P.; Devereaux, Z. Using Deposition Rate to Increase the Thermal and Kinetic Stability of Vapor-Deposited Hole Transport Layer Glasses Via a Simple Sublimation Apparatus. *J. Chem. Phys.* **2017**, *146*, 203328.
(60) Van den Brande, N.; Gujral, A.; Huang, C.; Bagchi, K.; Hofstetter, H.; Yu, L.; Ediger, M. D. Glass Structure Controls Crystal Polymorph Selection in Vapor-Deposited Films of 4, 4'-Bis (N-carbazolyl)-1, 1'-biphenyl. *Cryst. Growth Des.* **2018**, *18*, 5800−5807.
(61) Liu, T.; Cheng, K.; Salami-Ranjbaran, E.; Gao, F.; Li, C.; Tong, X.; Lin, Y.-C.; Zhang, Y.; Zhang, W.; Klinge, L.; Walsh, P. J.; Fakhraai, Z. The Effect of Chemical Structure on The Stability of Physical Vapor Deposited Glasses of 1,3,5-Triarylbenzene. *J. Chem. Phys.* **2015**, *143*, 084506.
(62) Ràfols-Ribé, J.; Gonzalez-Silveira, M.; Rodríguez-Tinoco, C.; Rodríguez-Viejo, J. The Role of Thermodynamic Stability in The Characteristics of The Devitrification Front of Vapour-Deposited Glasses of Toluene. *Phys. Chem. Chem. Phys.* **2017**, *19*, 11089−11097.
(63) Liu, T.; Exarhos, A. L.; Alguire, E. C.; Gao, F.; Salami-Ranjbaran, E.; Cheng, K.; Jia, T.; Subotnik, J. E.; Walsh, P. J.; Kikkawa, J.; Fakhraai, Z. Birefringent Stable Glass with Predominantly Isotropic Molecular Orientation. *Phys. Rev. Lett.* **2017**, *119*, 095502.
(64) Walters, D. M.; Antony, L.; de Pablo, J. J.; Ediger, M. D. Influence of Molecular Shape on The Thermal Stability and Molecular Orientation of Vapor-Deposited Organic Semiconductors. *J. Phys. Chem. Lett.* **2017**, *8*, 3380−3386.
(65) Gujral, A.; O'Hara, K. A.; Toney, M. F.; Chabinyc, M. L.; Ediger, M. Structural Characterization of Vapor-Deposited Glasses of an Organic Hole Transport Material With X-ray Scattering. *Chem. Mater.* **2015**, *27*, 3341−3348.
(66) Teerakapibal, R.; Huang, C.; Gujral, A.; Ediger, M. D.; Yu, L. Organic Glasses with Tunable Liquid-Crystalline Order. *Phys. Rev. Lett.* **2018**, *120*, 055502.
(67) Bagchi, K.; Jackson, N. E.; Gujral, A.; Huang, C.; Toney, M. F.; Yu, L.; de Pablo, J. J.; Ediger, M. D. Origin of Anisotropic Molecular Packing in Vapor-Deposited Alq3 Glasses. *J. Phys. Chem. Lett.* **2019**, *10*, 164−170.
(68) Singh, S.; Ediger, M. D.; De Pablo, J. J. Ultrastable Glasses From In Silico Vapour Deposition. *Nat. Mater.* **2013**, *12*, 139.
(69) Chen, Y.; Zhang, W.; Yu, L. Hydrogen Bonding Slows Down Surface Diffusion of Molecular Glasses. *J. Phys. Chem. B* **2016**, *120*, 8007−8015.
(70) Young-Gonzales, A.; Guiseppi-Elie, A.; Ediger, M.; Richert, R. Modifying Hydrogen-Bonded Structures by Physical Vapor Deposition: 4-Methyl-3-Heptanol. *J. Chem. Phys.* **2017**, *147*, 194504.
(71) Tylinski, M.; Beasley, M.; Chua, Y.; Schick, C.; Ediger, M. Limited Surface Mobility Inhibits Stable Glass Formation for 2-Ethyl-1-Hexanol. *J. Chem. Phys.* **2017**, *146*, 203317.
(72) Laventure, A.; Gujral, A.; Lebel, O.; Pellerin, C.; Ediger, M. Influence of Hydrogen Bonding on the Kinetic Stability of Vapor-Deposited Glasses of Triazine Derivatives. *J. Phys. Chem. B* **2017**, *121*, 2350−2358.
(73) Chen, Y.; Chen, Z.; Tylinski, M.; Ediger, M.; Yu, L. Effect of Molecular Size and Hydrogen Bonding on Three Surface-Facilitated Processes in Molecular Glasses: Surface Diffusion, Surface Crystal Growth, and Formation of Stable Glasses by Vapor Deposition. *J. Chem. Phys.* **2019**, *150*, 024502.
(74) Tylinski, M.; Chua, Y.; Beasley, M.; Schick, C.; Ediger, M. Vapor-Deposited Alcohol Glasses Reveal a Wide Range of Kinetic Stability. *J. Chem. Phys.* **2016**, *145*, 174506.
(75) Malshe, R.; Ediger, M.; Yu, L.; De Pablo, J. Evolution of Glassy Gratings With Variable Aspect Ratios Under Surface Diffusion. *J. Chem. Phys.* **2011**, *134*, 194704.
(76) Zhang, Y.; Fakhraai, Z. Invariant Fast Diffusion on The Surfaces of Ultrastable and Aged Molecular Glasses. *Phys. Rev. Lett.* **2017**, *118*, 066101.
(77) Liu, T.; Cheng, K.; Salami-Ranjbaran, E.; Gao, F.; Glor, E. C.; Li, M.; Walsh, P. J.; Fakhraai, Z. Synthesis and High-Throughput Characterization of Structural Analogues of Molecular Glassformers: 1, 3, 5-Trisarylbenzenes. *Soft Matter* **2015**, *11*, 7558−7566.
(78) Mullins, W. W. Flattening of a Nearly Plane Solid Surface Due to Capillarity. *J. Appl. Phys.* **1959**, *30*, 77−83.
(79) Adam, G.; Gibbs, J. H. On The Temperature Dependence of Cooperative Relaxation Properties in Glass-Forming Liquids. *J. Chem. Phys.* **1965**, *43*, 139−146.
(80) Hodge, I. Effects of Annealing and Prior History on Enthalpy Relaxation in Glassy Polymers. 6. Adam-Gibbs Formulation of Nonlinearity. *Macromolecules* **1987**, *20*, 2897−2908.
(81) Brian, C. W.; Zhu, L.; Yu, L. Effect of Bulk Aging on Surface Diffusion of Glasses. *J. Chem. Phys.* **2014**, *140*, 054509.
(82) Rodríguez-Tinoco, C.; Gonzalez-Silveira, M.; Ràfols-Ribé, J.; Garcia, G.; Rodríguez-Viejo, J. Highly Stable Glasses of Celecoxib: Influence on Thermo-Kinetic Properties, Microstructure and Response Towards Crystal Growth. *J. Non-Cryst. Solids* **2015**, *407*, 256−261.
(83) Glor, E. C.; Fakhraai, Z. Facilitation of Interfacial Dynamics in Entangled Polymer Films. *J. Chem. Phys.* **2014**, *141*, 194505.
(84) Peter, S.; Meyer, H.; Baschnagel, J. Thickness-Dependent Reduction of The Glass-Transition Temperature in Thin Polymer Films With a Free Surface. *J. Polym. Sci., Part B: Polym. Phys.* **2006**, *44*, 2951−2967.
(85) Lam, C.-H. Deeper Penetration of Surface Effects on Particle Mobility Than on Hopping Rate in Glassy Polymer Films. *J. Chem. Phys.* **2018**, *149*, 164909.
(86) Zhang, Y.; Glor, E. C.; Li, M.; Liu, T.; Wahid, K.; Zhang, W.; Riggleman, R. A.; Fakhraai, Z. Long-Range Correlated Dynamics in Ultra-Thin Molecular Glass Films. *J. Chem. Phys.* **2016**, *145*, 114502.

DOI: 10.1021/acs.jpcb.9b01012
J. Phys. Chem. B 2019, 123, 4108−4117